from 2853 to 2857 cm^{-1} indicates increased numbers of gauche conformers from which a larger amount of conformational disorder of the lipid chains may be inferred.[25] The decrease in the acyl chain double bond C-H stretching mode intensity at 3013 cm^{-1} in the complex demonstrates the involvement and possibly change in the surrounding environment of the cis double bonds at the 9-10 and 11-12 positions of the lipid chains. The participation of these regions of the lipid chains in complex formation strongly suggests that this lipid binding involves substantial conformational changes within the acyl chains and that the binding consists of more than a simple attraction of the negatively charged lipid head groups with the positively charged lysines ringing the heme crevice in the protein.

In summary, complexation of ferricytochrome *c* with cardiolipin modifies the structure of the heme group to mimic the heme conformation of the reduced ferrocytochrome *c* species, while not affecting the iron oxidation state. The reduction potential for the cardiolipin complex of ferricytochrome *c* is altered from 273 mV for the uncomplexed cytochrome *c* to 225 mV for the bound system.[26] The presence of cardiolipin in the inner mitochondrial membrane and the ease with which cardiolipin forms a complex with cytochrome *c* suggest that this specific lipid-protein complex may be important in clarifying the functional roles of the protein. In view of the structural changes observed for cytochrome *c* in these studies, it is important to assign oxidation states of heme or porphyrin systems with extreme care when using resonance Raman spectra as guides.

Acknowledgment. We thank Dr. H. Kon for considerable aid in obtaining the electron paramagnetic resonance data. We also wish to thank Dr. Richard Hendler for the use of his visible spectrometer and for numerous helpful discussions. J.S.V. acknowledges receipt of an NIH Senior National Research Service Award.

Registry No. Cytochrome *c*, 9007-43-6.

(25) Snyder, R. G.; Strauss, H. L.; Ellinger, C. A. *J. Phys. Chem.* **1982**, *86*, 5145-5150.

(26) Kimelberg, H. K.; Lee, C. P. J. *Membr. Biol.* **1970**, *2*, 252-262.

(27) TRIS, tris(hydroxymethyl)aminomethane. HEPES, *N*-(2-hydroxyethyl)piperazine-*N'*-2-ethanesulfonic acid.

Interaction of Ethylene with the Ru(001) Surface†

M. M. Hills, J. E. Parmeter,‡ C. B. Mullins,§ and W. H. Weinberg*

Contribution from the Division of Chemistry and Chemical Engineering, California Institute of Technology, Pasadena, California 91125. *Received October 8, 1985*

Abstract: The interaction of ethylene with the Ru(001) surface has been investigated via high-resolution electron energy loss spectroscopy and thermal desorption mass spectrometry. Following desorption of an ethylene multilayer at 110 K, di-σ-bonded molecular ethylene is present on the surface. Competing desorption of molecular ethylene and dehydrogenation to form adsorbed ethylidyne (CCH_3) and acetylide (CCH) as well as hydrogen adatoms occur between approximately 150 and 260 K. The ethylidyne is stable to approximately 330 K, whereupon it begins to decompose to carbon and hydrogen adatoms. The desorption of hydrogen occurs in a sharp peak centered at 355 K, resulting from simultaneous ethylidyne decomposition and desorption of surface hydrogen. Further annealing of the overlayer to 380 K causes cleavage of the carbon-carbon bond of the acetylide, creating carbon adatoms and adsorbed methylidyne (CH). The methylidyne decomposes above 500 K with accompanying hydrogen desorption, leaving only carbon adatoms on the surface at 700 K.

I. Introduction

The adsorption and reaction of ethylene on single crystalline surfaces of the groups 8-10 transition metals[1-17] have been the subject of intense study both as a prototype for olefin hydrogenation and dehydrogenation reactions[18-21] and to provide a basis for comparing the bonding of olefins to surfaces with the bonding that has been observed to occur in multinuclear organometallic cluster compounds. Spectroscopic studies of ethylene adsorbed on these surfaces have shown that both the nature of the bonding of molecular ethylene to the substrate as well as the thermal decomposition pathway of the adsorbed ethylene vary widely. For example, ethylene rehybridizes to a di-σ-bonded molecular species when adsorbed on Fe(110), Fe(111), Ni(110), Ni(111), Ni[5(111) × (110)], Pt(111), and Pt(100),[1-7] whereas molecularly adsorbed ethylene on Co(001) at 115 K is π-bonded,[8] as is ethylene adsorbed on Pd(111) at 150 K and on Pd(110) at 110 K.[6,9-13,17] A mixed overlayer of π- and di-σ-bonded ethylene forms on Pd(100) at 150 K.[14,15] Ethylene adsorption on the Ru(001) surface has been

† In this paper the periodic group notation in parentheses is in accord with recent actions by IUPAC and ACS nomenclature committees. A and B notation is eliminated because of wide confusion. Groups IA and IIA become groups 1 and 2. The d-transition elements comprise groups 3 through 12, and the p-block elements comprise groups 13 through 18. (Note that the former Roman number designation is preserved in the last digit of the numbering: e.g., III → 3 and 13.)

‡ AT&T Bell Laboratories predoctoral fellow.

§ Link Foundation predoctoral fellow.

(1) Erley, W.; Baro, A. M.; McBreen, P.; Ibach, H. *Surf. Sci.* **1982**, *120*, 273.
(2) Seip, U.; Tsai, M.-C.; Küppers, J.; Ertl, G. *Surf. Sci.* **1984**, *147*, 65.
(3) Stroscio, J. A.; Bare, S. R.; Ho, W. *Surf. Sci.* **1984**, *148*, 499.
(4) Lehwald, S.; Ibach, H. *Surf. Sci.* **1979**, *89*, 425.
(5) Carr, R. G.; Sham, T. K.; Eberhardt, W. E. *Chem. Phys. Lett.* **1985**, *113*, 63.
(6) Demuth, J. E. *Surf. Sci.* **1979**, *84*, 315.
(7) Steininger, H.; Ibach, H.; Lehwald, S. *Surf. Sci.* **1982**, *117*, 685.
(8) Albert, M. R.; Sneddon, L. G.; Plummer, E. W. *Surf. Sci.* **1984**, *147*, 127.
(9) Gates, J. A.; Kesmodel, L. L. *Surf. Sci.* **1982**, *120*, L461.
(10) Gates, J. A.; Kesmodel, L. L. *Surf. Sci.* **1983**, *124*, 68.
(11) Tysoe, W. T.; Nyberg, G. L.; Lambert, R. M. *J. Phys. Chem.* **1984**, *88*, 1960.
(12) Ratajczykowa, I.; Szymerska, I. *Chem. Phys. Lett.* **1983**, *96*, 243.
(13) Kesmodel, L. L.; Gates, J. A. *Surf. Sci.* **1981**, *111*, L747.
(14) Stuve, E. M.; Madix, R. J. *J. Phys. Chem.* **1985**, *89*, 105.
(15) Stuve, E. M.; Madix, R. J.; Brundle, C. R. *Surf. Sci.* **1985**, *152/153*, 532.
(16) Dubois, L. H.; Castner, D. G.; Somorjai, G. A. *J. Chem. Phys.* **1980**, *72*, 5234.
(17) Gupta, N. M.; Kamble, V. S.; Iyer, R. M. *J. Catal.* **1984**, *88*, 457.
(18) Chesters, M. A.; McDougall, G. S.; Pemble, M. E.; Sheppard, N. *Appl. Surf. Sci.* **1985**, *22/23*, 369.
(19) Boudart, M.; McDonald, M. A. *J. Phys. Chem.* **1984**, *88*, 2185.
(20) Henrici-Olivé, G.; Olivé, S. *Angew. Chem., Int. Ed. Engl.* **1976**, *15*, 136.

0002-7863/86/1508-3554$01.50/0

studied recently by Barteau and co-workers.[22] A detailed comparison between our more complete study and the preliminary results of Barteau et al.[22] is presented in section IV.

The thermal decomposition of ethylene (ultimately to hydrogen and surface carbon) on the surfaces mentioned above has been investigated by vibrational electron energy loss spectroscopy (EELS), thermal desorption mass spectrometry (TDMS), and UV photoelectron spectroscopy. The thermal decomposition intermediates in ethylene dehydrogenation on Fe(110), Ni(111), Ni[5(111) × (110)], and Ni(110) are acetylene and acetylide (CCH).[1,3,4] Madix and Stuve have postulated the formation of a vinyl group from ethylene adsorbed on Pd(100).[14,15] On Co(001) and Fe(111) no stable surface intermediates were observed; chemisorbed ethylene evidently dehydrogenates completely just below room temperature to carbon and hydrogen.[2,8] On Pt(111), Rh(111), Pd(111), and Pt(100), chemisorbed ethylene dehydrogenates to form ethylidyne below 300 K.[7,9-13,16,23] Thus, ethylene adsorbed on the close-packed surfaces of each of the 4d and 5d groups 8–10 metals studied previously forms ethylidyne.[24] On the other hand, ethylene adsorbed on all of the surfaces of the 3d groups 8–10 metals studied to date, including the close-packed surfaces, dehydrogenates more completely to acetylene, acetylide, or directly to carbon. Hence it is of fundamental interest to determine whether ethylene adsorbed on the Ru(001) surface behaves as it does on the other hexagonal 4d and 5d transition-metal surfaces studied previously [Rh(111), Pd(111), Pt(100), and Pt(111)] or whether it dehydrogenates more completely, as it does on the hexagonal Ni(111) and Co(001) surfaces.

II. Experimental Procedures

The experimental measurements were conducted in two different ultrahigh-vacuum (UHV) chambers, each with base pressures below 1 × 10^{-10} torr. The first UHV chamber is equipped with a quadrupole mass spectrometer, a single pass cylindrical mirror electron energy analyzer with an integral electron gun for Auger electron spectroscopy, and LEED optics. All thermal desorption measurements were carried out in this chamber; data were collected by using an LSI-11 DEC laboratory computer, and linear heating rates of 5–15 K/s were employed. A glass enclosure is placed around the ionizer of the mass spectrometer, and a small aperture in the front of the glass envelope permits sampling of gas that is desorbed only from the well-oriented front of the single crystal. Thus the effects of desorption from the edge of the crystal, the support leads, and the manipulator are excluded from the thermal desorption spectra.[26]

The second UHV chamber contains both a quadrupole mass spectrometer and a home-built EELS spectrometer of the Kuyatt-Simpson type.[27,28] The energy dispersing elements in the EELS monochromator and rotatable analyzer are 180° hemispherical deflectors. The "off-specular" EEL spectra were measured with the analyzer rotated 7–10° from the specular direction, toward the surface normal. All EEL spectra were measured using a beam energy of 4 eV and with the incident beam approximately 60° from the surface normal. The instrumental resolution (full-width at half-maximum of the elastically scattered peak) varied between 60 and 80 cm^{-1}, while maintaining a count rate of approximately 3 × 10^5 cps in the elastic peak. A more extensive description of these UHV chambers as well as the procedures followed for cutting, polishing, mounting, and cleaning the Ru(001) crystals has been discussed in detail previously.[27-30] The cleanliness of the surfaces was monitored with Auger spectroscopy in the first chamber and with EELS in the second.

Research purity hydrogen (99.9995%) and C.P. grade deuterium and ethylene (99.5%) were purchased from Matheson. Research purity tetradeuterated ethylene (99.99%) was obtained from Merck. The H_2, D_2, and C_2D_4 were used without further purification, whereas the C_2H_4 was subjected to freeze–thaw–pump cycles prior to use. The purity of all gases was verified in situ with mass spectrometry.

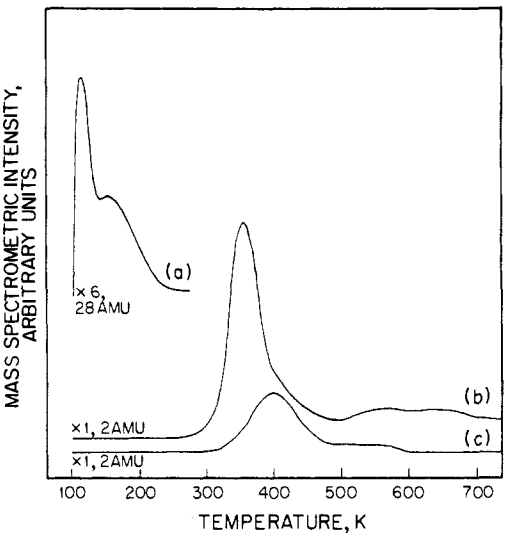

Figure 1. Thermal desorption spectra after C_2H_4 adsorption on Ru(001) at 90 K: (a) C_2H_4 and (b) H_2 desorption following a 1-langmuir exposure and (c) H_2 desorption following a 0.2-langmuir exposure.

III. Results

Typical thermal desorption spectra following exposure of the Ru(001) surface to 1 langmuir (1 langmuir = 1 × 10^{-6} torr s) or more of C_2H_4 at 90 K are shown in Figure 1a and 1b.[31] Only hydrogen and ethylene are observed to desorb from the surface. In particular, no ethane, methane, or acetylene is detected as judged by the absence of 30 and 16 amu peaks and by comparison of the 28, 27, and 26 amu peaks to the cracking pattern of ethylene.

Figure 1b establishes that most of the hydrogen, after an ethylene exposure exceeding 0.6 langmuir, desorbs in a sharp peak centered at 355 K (independent of coverage), with a small high-temperature shoulder above 400 K and a broad tail extending from 500 to 700 K of which the latter represents 10–15% of the desorbing hydrogen. It will be shown below that the major peak corresponds to the desorption of hydrogen enhanced by the decomposition of ethylidyne (one of the decomposition products of ethylene), the shoulder corresponds to desorption-limited hydrogen from the surface, and the high-temperature tail corresponds to the dehydrogenation of surface methylidyne (another decomposition product). The thermal desorption spectrum of molecular ethylene (cf. Figure 1a) shows that ethylene desorbs in a sharp peak centered near 110 K, followed by a broad peak of which the tail extends to approximately 250 K. As discussed below, EEL spectra of the surface on which ethylene is adsorbed and which is annealed to various temperatures show that the higher-temperature peak corresponds to the desorption of di-σ-bonded ethylene, while multilayer ethylene desorbs in the lower-temperature peak. The "multilayer" peak shown in Figure 1a actually corresponds to only desorption from a second layer. This multilayer peak does not saturate with increasing ethylene exposure, however, and is sufficiently intense following a 15-langmuir exposure of ethylene that it obscures the desorption peak due to chemisorbed ethylene.

For lower exposures of ethylene, below 0.6 langmuir, the hydrogen thermal desorption spectra are quite different. The thermal desorption spectrum of H_2 after an ethylene exposure of 0.2 langmuir, shown in Figure 1c, contains a high-temperature tail terminating below 600 K that is due to methylidyne decomposition and a rather broad peak centered at 420 K that shifts to lower temperature as the initial surface coverage of chemisorbed ethylene increases. The latter is essentially identical with that which is observed after adsorption of hydrogen on the clean Ru(001) surface.[32] The maximum rate of H_2 desorption shifts from 420

(21) Dixit, R. S.; Tavlarides, L. L. *Ind. Eng. Chem. Process Des. Dev.* **1983**, *22*, 1.
(22) Barteau, M. A.; Broughton, J. Q.; Menzel, D. *Appl. Surf. Sci.* **1984**, *19*, 92.
(23) Ibach, H. Presented at the Proceedings of the International Conference on Vibrations in Adsorbed Layers, Julich, 1978; paper 64.
(24) The Pt(100) surface reconstructs to a slightly buckled, close-packed (5 × 20) superstructure.[25]
(25) Heilmann, P.; Heinz, K.; Müller, K. *Surf. Sci.* **1979**, *83*, 487.
(26) Feulner, P.; Menzel, D. *J. Vac. Sci. Technol.* **1980**, *17*, 662.
(27) Thomas, G. E.; Weinberg, W. H. *Phys. Rev. Lett.* **1978**, *418* 1181.
(28) Thomas, G. E.; Weinberg, W. H. *Rev. Sci. Instrum.* **1979**, *50*, 497.
(29) Williams, E. D.; Weinberg, W. H. *Surf. Sci.* **1979**, *82*, 93.
(30) Williams, E. D.; Weinberg, W. H. *J. Vac. Sci. Technol.* **1982**, *20*, 534.
(31) All exposures reported are uncorrected for the sensitivity of the ion gauge to the various gases.
(32) Shimizu, H.; Christmann, K.; Ertl, G. *J. Catal.* **1980**, *61*, 412.

Table I. Comparison of Vibration Frequencies of Multilayer C_2H_4 Adsorbed on Ru(001) at 80 K with C_2H_4(g), C_2H_4(l), and C_2H_4(s)[a]

		C_2H_4(g)[33]		C_2H_4(l)[34]		C_2H_4(s)[34]	multilayer C_2H_4
no/repr.	mode	Raman	IR	Raman	IR	IR	on Ru(001)
ν_1 A_g	$\nu_s(CH_2)$	3026	f	3019	3016		3000
ν_{11} B_{2u}		f	2989		2983	2973	
ν_5 B_{1g}	$\nu_a(CH_2)$	3103	f	3075			3095
ν_9 B_{2u}		f	3105		3085	3075	
ν_2 A_g	ν(CC)	1623	f	1621	1620	1616	1630
ν_3 A_g	CH_2 scis.	1342	f	1340	1339	1336	1350
ν_{12} B_{3u}		f	1444		1437	1438	1460
ν_4 A_u	CH_2 twist	f	f		~1010		n.r.
ν_6 B_{1g}	CH_2 rock		f	1236	1239		
ν_{10} B_{2u}		f	810		828	827	860
ν_7 B_{1u}	CH_2 wag	f	949		960	970	970
ν_8 B_{2g}		950	f	943			
	ν_s(RuC)						440

no./repr.	mode	C_2D_4(g)[33]	multilayer C_2D_4 on Ru(001)
ν_1 A_g	$\nu_s(CD_2)$	2251	2310
ν_{11} B_{2u}		2200	
ν_5 B_{1g}	$\nu_a(CD_2)$	2304	n.r.
ν_9 B_{2u}		2345	
ν_2 A_g	ν(CC)	1515	1550
ν_3 A_g	CD_2 scis.	981	1015
ν_{12} B_{3u}		1078	1175
ν_4 A_u	CD_2 twist	728	n.r.
ν_6 B_{1g}	CD_2 rock	1009	n.r.
ν_{10} B_{2u}		586	
ν_7 B_{1u}	CD_2 wag	720	735
ν_8 B_{2g}		780	
	ν_s(RuC)		425

[a] n.r. = nor resolved. f = forbidden.

K for an ethylene exposure of 0.2 langmuir to 395 K for a 0.4-langmuir exposure and then drops to 355 K for all ethylene exposures exceeding 0.6 langmuir. The decrease in peak temperature for exposures of ethylene below 0.6 langmuir is indicative of second-order desorption kinetics of surface hydrogen. For these lower exposures of ethylene, below 0.6 langmuir, no desorption of molecular ethylene is observed.

Figure 2a and 2b shows the EEL spectra of 4 langmuir of C_2H_4 and 3 langmuir of C_2D_4, respectively, adsorbed at 80 K on the Ru(001) surface. Consistent with the thermal desorption spectra, a comparison of the observed energy loss features to IR and Raman spectra of gaseous, liquid, and solid ethylene (cf. Table I[33,34]) demonstrates that the overlayers of Figure 2 correspond to molecular multilayers. Note the intense CH_2 wagging mode at 970 cm^{-1}, which is the best fingerprint of molecular ethylene multilayers, and also the carbon–hydrogen stretching mode at 3000 cm^{-1}. The frequencies of both these modes are characteristic of an sp^2-hybridized carbon atom. Table I also shows that the isotopic shifts for multilayer C_2D_4 on Ru(001) are in good agreement with those of C_2D_4(g).

Annealing these overlayers to 110 K desorbs the multilayer, as shown in the thermal desorption spectra (cf. Figure 1a), leaving di-σ-bonded ethylene which is stable to 150 K. The EEL spectra of this chemisorbed species are exhibited in Figure 3a for C_2H_4 and Figure 3b for C_2D_4. The rehybridization of the carbon atoms to nearly sp^3 is reflected in the shifts of the CH_2 wagging mode and the carbon–hydrogen stretching mode to 1145 and 2985 cm^{-1}, respectively. The shoulder at 1040 cm^{-1} is probably due to the carbon–carbon stretching mode, but it is poorly resolved from the CH_2 twisting mode in C_2H_4 and the CD_2 wagging mode in C_2D_4 both of which are at 900 cm^{-1}. A carbon–carbon stretching frequency of 1040 cm^{-1} is consistent with the rehybridization of the carbon atoms of ethylene to sp^3. Other modes of di-σ-bonded

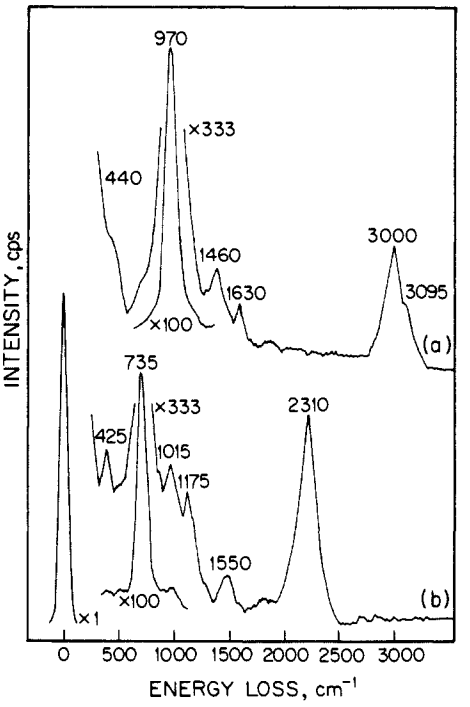

Figure 2. EEL spectra of molecular multilayers of ethylene on Ru(001): (a) 4 langmuir of C_2H_4 at 80 K and (b) 3 langmuir of C_2D_4 at 80 K.

ethylene are the symmetric ruthenium–carbon stretching mode at 460 cm^{-1} (420 cm^{-1} for C_2D_4), the CH_2 rocking mode at 775 cm^{-1}, the CH_2 twisting mode at 900 cm^{-1} (700 cm^{-1} for C_2D_4), and the CH_2 scissoring mode at 1450 cm^{-1} (1210 cm^{-1} for C_2D_4). The CD_2 rocking mode of di-σ-bonded C_2D_4 was not resolved in Figure 3b due to the poorer cutoff in the elastic peak. The symmetric ruthenium–carbon stretching mode of di-σ-bonded

(33) Shimanouchi, T. *NSRDS-NBS* **1972**, *39*, 74.
(34) Brecher, C.; Halford, R. S. *J. Chem. Phys.* **1961**, *35*, 1109.

Table II. Comparison of Vibrational Frequencies of Di-σ-bonded C_2H_4 on Ru(001) at 130 K with Other Chemisorbed Ethylene Species, Gaseous Ethylene Compounds, Organometallic Ethylene Compounds, and a Surface Methylene Species[a]

	di-σ-C_2H_4 on							gauche			
	Ru(001)	Ni(110)[3]	Ni(111)[4]	Fe(110)[1]	Fe(111)[2]	Pt(111)[7]	C_2H_4(g)[33]	$C_2H_4Br_2$(g)[33]	$K[PtCl_3$-$(C_2H_4)]H_2O$[35]	Ni_2-$(C_2H_4)_4$[36]	CH_2 on Ru(001)[38]
mode C_2H_4 (or CH_2)											
ν_s(CM)	460	420	450	480	580	470				376	n.r.
ν_a(CM)	n.r.	n.r.	610	410	450	560					n.r.
CH_2 rock	775	715	720	720	n.r.	660	826	848	841	910	785
CH_2 twist	900	850	880	915	870	790	f	1104			
CH_2 wag	1145	1145	1110	1105	n.r.	980	949	1278	975	1180	1155
CH_2 scissors	1450	1435	1430	1410	1385	1430	1444	1420	1515	1208	
$\nu_s(CH_2)$	2940	2970	2930	2960	2980	2980	2989	2953	3013	2880	2965
$\nu_a(CH_2)$	3050	n.r.	n.r.	n.r.	n.r.	3000	3096	3005	3075	2908	n.r.
ν(CC)	1040	n.r.	1200	1250	1115	1060	1623	1019	1243	1488	
mode C_2D_4											
ν_s(CM)	420	390	420	440		450					
ν_a(CM)	n.r.	n.r.	590	n.r.		n.r.					
CD_2 rock	n.r.	615	650	635/540		n.r.	586	712			
CD_2 twist	700	725	740	700		600	f	791			
CD_2 wag	900	925	870	850		740	720	947			
CD_2 scissors	1210	1235	1200	1040		1150	1078	1141			
$\nu_s(CD_2)$	2210	2170	2170	2175		2150	2251	2174			
$\nu_a(CD_2)$	2295	2290	2270	n.r.		2250	2304	2271			
ν(CC)	n.r.	n.r.	n.r.	1160		900	1515	1014			

[a] f = forbidden. n.r. = not resolved.

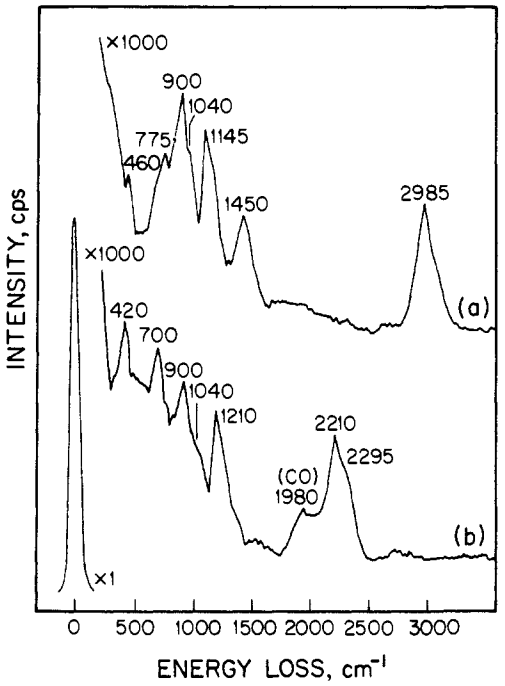

Figure 3. EEL spectra of di-σ-bonded ethylene on Ru(001): (a) 4 langmuir of C_2H_4 annealed to 139 K and (b) 3 langmuir of C_2D_4 annealed to 123 K.

C_2D_4 also contains a small contribution from ν(Ru–CO). The symmetric and asymmetric carbon–hydrogen stretching modes of C_2H_4 at 2940 and 3050 cm^{-1} were resolved in spectra similar to Figure 3a.

Peak assignments for di-σ-bonded ethylene (both C_2H_4 and C_2D_4) on Ru(001) are compared in Table II with those of other chemisorbed ethylene species as well as IR data for $C_2H_4Br_2$(g), C_2H_4(g), Zeise's salt, and a low-valent nickel complex $[Ni(C_2H_4)_n]$.[1-4,7,33,35,36] A comparison of the frequencies of the modes of di-σ-bonded C_2H_4 on Ru(001) to these data shows that ethylene undergoes rehybridization on the Ru(001) surfaces as on Ni(110), Ni(111), and Fe(110).[1,3-5] The existence of a π-bonded ethylene admolecule can be excluded by a comparison to the IR data for Zeise's salt and Ozin's nickel complexes, which have, among other differences, higher frequency CH_2 rocking modes and carbon–carbon stretching modes.

A comparison of EEL spectra of di-σ-bonded ethylene with spectra of diazomethane led to an original assignment of the spectrum of Figure 3a as a bridging methylene species.[37] However, a subsequent review of these and other spectra has shown that the reaction of CH_2N_2 to form C_2H_4 and N_2 may occur in the gas dosing lines prior to introduction into the UHV chamber. An assignment of EEL spectra of uncontaminated diazomethane, which produces μ_2-CH_2 groups on Ru(001), is listed in the last column in Table II. Additional vibrational data concerning bridging methylene may be found elsewhere.[39-43] The adsorption of C_2H_4 on Ru(001) with annealing to 110 K produces di-σ-bonded molecular ethylene, which can be distinguished from μ_2-CH_2 by the intense CH_2 twisting mode at 900 cm^{-1}. In agreement with this conclusion, the thermal desorption spectra of ethylene on Ru(001) show desorption of molecular ethylene up to 250 K.

In an effort to describe further the character of the di-σ-bonded ethylene on Ru(001), isotopic exchange, thermal desorption experiments of coadsorbed C_2H_4 and C_2D_4 were carried out. In all cases, only C_2H_4 and C_2D_4 desorbed from the multilayer. However, all five isotopically labeled species (C_2H_4, C_2H_3D, $C_2H_2D_2$, C_2HD_3, and C_2D_4) appeared in the di-σ-bonded ethylene that desorbs molecularly. Figure 4 shows the relative ratios of these five species that desorb molecularly above 150 K. These ratios were obtained by correcting the areas under the thermal desorption peaks of the 26–32-amu spectra, both for the cracking patterns of the five species and for the relative sensitivity of the mass spectrometer to each species. (These ratios *exclude* multilayer C_2H_4 and C_2D_4.) Figure 4 shows that isotopic exchange is limited, and no mixed species (C_2H_3D, $C_2H_2D_2$, or C_2HD_3) is favored over the other two. On the other hand, the corresponding $H_2/HD/D_2$ thermal desorption spectra exhibited complete isotopic exchange. The above results suggest that the isotopic mixing observed for

(35) Hiraishi, J. *Spectrochim. Acta, Part A* **1969**, *25A*, 749.
(36) Ozin, G. A. *J. Am. Chem. Soc.* **1978**, *100*, 4750.
(37) George, P. M.; Avery, N. R.; Weinberg, W. H.; Tebbe, F. N. *J. Am. Chem. Soc.* **1983**, *105*, 1393.
(38) EEL spectra of 2.5 langmuir of H_2CN_2 dosed at 80 K, annealed to 192–316 K, and cooled to 80 K prior to measurement.
(39) Fox, D. J.; Schaefer, H. F. *J. Chem. Phys.* **1983**, *78*, 328.
(40) Theopold, K. H.; Bergman, R. G. *J. Am. Chem. Soc.* **1981**, *103*, 2489.
(41) Oxton, I. A.; Powell, D. B.; Sheppard, N.; Burgess, K.; Johnson, B. F. G.; Lewis, J. *Chem. Soc., Chem. Commun.* **1982**, 719.
(42) McBreen, P. H.; Erley, W.; Ibach, H. *Surf. Sci.* **1984**, *148*, 292.
(43) Chang, S.-C.; Kafafi, Z. H.; Hauge, R. H.; Billups, W. E.; Margave, J. L. *J. Am. Chem. Soc.* **1985**, *107*, 1447.

Table III. Comparison of Vibrational Frequencies of Ethylidyne

mode	CCH_3 on Ru(001) at 280 K	CCH_3 on Pd(111) at 300 K[4]	CCH_3 on Pt(111) at 300 K[7]	CCH_3 on Rh(111) at 300 K[16]	$(CO)_9Co_3(\mu_3\text{-}CCH_3)$[45]
ν_s(CM) A_1	480[b]	409	435 vs	450	401
ν_a(CM) E	n.r.[a]	n.r.	600 w	n.r.	555
ρ(CH_3) E	1000	n.r.	980 sh	n.r.	1004
ν(CC) A_1	1140	1080 s	1130 vs	1130	1163
δ_s(CH_3) A_1	1370	1334 vs	1355 vs	1350	1356
δ_a(CH_3) E	1450	1400	1420 sh	n.r.	1420
ν_s(CH_3) A_1	2945	2900 m	2920	2900	2888
ν_a(CH_3) E	3045	n.r.	3050	3000	2930
			Deuterated Species		
ν_s(CM) A_1	480	n.r.	410		393
ν_a(CM) E	n.r.	n.r.	~600		536
ρ(CD_3) E	800	n.r.	790		828
ν(CC) A_1	1150	1120	1160		1182
δ_s(CD_3) A_1	1000	n.r.	990		1002
δ_a(CD_3) E	n.r.	n.r.	1030		1031
ν_s(CD_3) A_1	2190	2181	2080		n.r.
ν_a(CD_3) E	2280	n.r.	2220		2192

[a] n.r. = not resolved. [b] Identified from spectra similar to that of Figure 5a but without CO contamination.

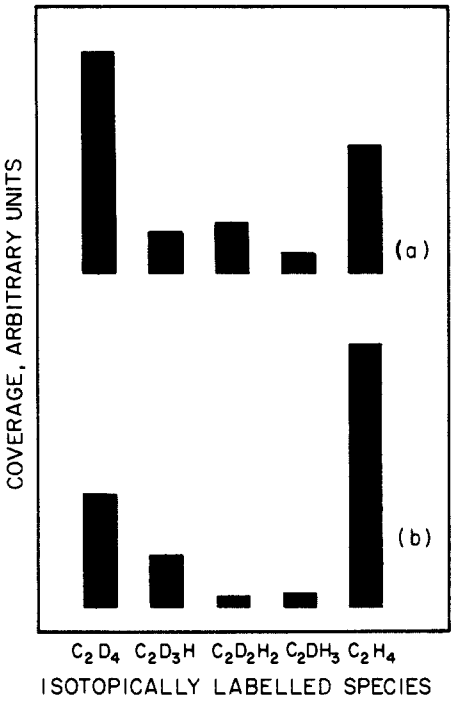

Figure 4. Coadsorption of C_2H_4 and C_2D_4. Relative coverages of C_2H_4, C_2H_3D, $C_2H_2D_2$, C_2HD_3, and C_2D_4 from thermal desorption spectra: (a) 0.6-langmuir exposure of C_2H_4 followed by 3 langmuir of C_2D_4 at 110 K and (b) 1-langmuir exposure of C_2H_4 followed by 3 langmuir of C_2D_4 at 110 K.

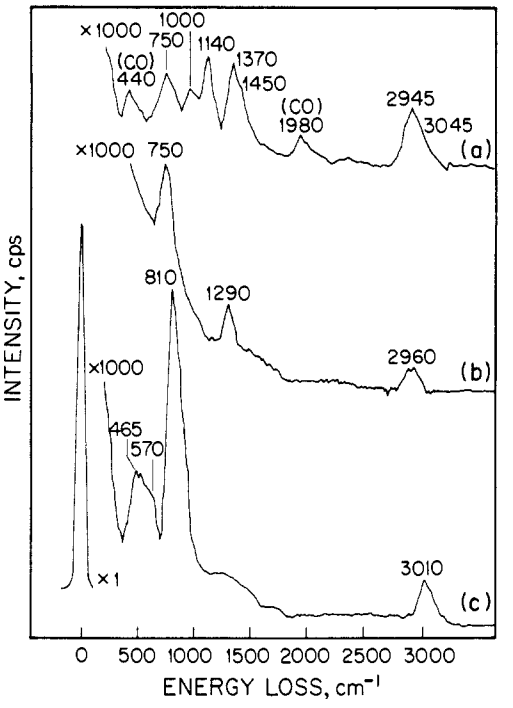

Figure 5. EEL spectra of 4 langmuir of C_2H_4 adsorbed on Ru(001) at 80 K and annealed to (a) 280, (b) 360, and (c) 500 K. Spectrum a exhibits the modes of both ethylidyne and acetylide. Spectrum b is characteristic of acetylide. Spectrum c corresponds to methylidyne.

chemisorbed ethylene that desorbs molecularly results from exchange between an ethylene admolecule and a hydrogen (or deuterium) adatom, since the onset of desorption of the mixed molecular ethylene species ($C_2H_xD_{4-x}$, $1 \le x \le 3$) coincides with the initial decomposition of ethylene to ethylidyne, acetylide, and surface hydrogen via carbon–hydrogen bond cleavage.

Annealing di-σ-bonded ethylene to 250 K produces two new carbon-containing surface species as well as hydrogen adatoms. The modes due to surface hydrogen were not resolved in the corresponding EEL spectrum shown in Figure 5a. The weak losses of hydrogen adatoms, which occur at 845 and 1115 cm^{-1},[44] were obscured by various carbon–hydrogen and carbon–carbon modes. However, the presence of hydrogen adatoms was confirmed by stoichiometric considerations and hydrogen postadsorption experiments which will be discussed later. The two hydrocarbon fragments present on the surface have been identified as ethylidyne and acetylide from the EEL spectrum of Figure 5a, the corresponding EEL spectrum of the deuterated species, off-specular EELS measurements, and EEL spectra measured following annealing to various temperatures.

Peak assignments for CCH_3 and CCD_3 are compared in Table III to IR data for a tricobalt ethylidyne complex as well as EELS results for ethylidyne adsorbed on various close-packed groups 8–10 metal surfaces.[4,7,16,45] A triruthenium ethylidyne complex has also been synthesized, but no relevant IR data have been published.[46] For all of the ethylidyne adspecies listed in Table III, the carbon–carbon stretching mode produces a strong, dipolar enhanced peak. By analogy to the structure of the triruthenium and tricobalt organometallic compounds, and considering the relative intensities of the (dipolar-enhanced) carbon–carbon stretching modes, the carbon–carbon bond axis of each of the

(44) Barteau, M. A.; Broughton, J. Q.; Menzel, D. *Surf. Sci.* **1983**, *133*, 443.

(45) Skinner, P.; Howard, M. W.; Oxton, I. A.; Kettle, S. F. A.; Powell, D. B.; Sheppard, N. *J. Chem. Soc., Faraday Trans 2* **1981**, *77*, 1203.

(46) Sheldrick, G. M.; Yesinowski, J. P. *J. Chem. Soc., Dalton Trans* **1975**, 873.

Table IV. Comparison of Vibrational Frequencies of Acetylide[a]

mode	CCH on Ru(001) at 360 K	CCH on Pd(100) at 400 K[48,49]
ν_s(CM)	435	n.r.
ν_a(CM)	n.r.	n.r.
δ(CH)	750	750
ν(CH)	2960	3000
ν(CC)	1290	1340
mode	**CCD**	**CCD**
ν_s(CM)	n.r.	n.r.
ν_a(CM)	n.r.	n.r.
δ(CD)	550	540
ν(CD)	2210	2220
ν(CC)	1260	1340

[a] n.r. = not resolved.

ethylidyne adspecies is nearly perpendicular to the surface plane. A comparison of the EELS losses for CCH_3 and CCD_3 on Ru(001) with IR data for $(CO)_9Co_3(\mu_3\text{-}CCH_3)$ and $(CO)_9Co_3(\mu_3\text{-}CCD_3)$ (cf. Table III) shows that the structure and bonding of the ethylidynes in the two cases are quite similar.

The acetylide species is characterized by a carbon–hydrogen bending mode at 750 cm^{-1}, a carbon–hydrogen stretching mode at 2960 cm^{-1}, and a carbon–carbon stretching mode at 1290 cm^{-1}. The vibrational modes of acetylide are partially obscured by the ethylidyne modes because the ratio of ethylidyne to acetylide present in Figure 4a is approximately 3:2, on the basis of hydrogen thermal desorption measurements. Annealing this overlayer to 360 K decomposes the ethylidyne, leaving acetylide, carbon, and a small concentration of hydrogen adatoms on the surface. Thus the modes of the acetylide are completely resolved in spectra measured after annealing the overlayer to 360 K (cf. Figure 5b). This acetylide also forms from the thermal decomposition of acetylene and is discussed in greater detail in the following paper.[47] We merely note here that these assignments agree quite well with those of Kesmodel et al. for acetylide on Pd(100) for which δ(CH) is 750 cm^{-1}, ν(CC) is 1340 cm^{-1}, and ν(CH) is 3000 cm^{-1},[48,49]

The EEL spectra of the deuterated acetylide show that the carbon–deuterium bending mode of CCD downshifts to 550 cm^{-1} from 750 cm^{-1} for CCH (cf. Table IV), which compares well with the value of δ(CD) of 540 cm^{-1} for CCD on Pd(100).[48,49] We also observe a slight shift in ν(CC) from 1290 cm^{-1} in CCH to 1260 cm^{-1} in CCD and the expected shift in ν(CD) from 2960 cm^{-1} in CCH to approximately 2210 cm^{-1} in CCD. These losses persist up to 380 K where cleavage of the carbon–carbon bond of the acetylide occurs, forming surface carbon and methylidyne.

The adsorbed methylidyne is identified from the EEL spectrum of Figure 5c with ν(RuC) at 465 cm^{-1}, δ(RuCH) at 810 cm^{-1}, and ν(CH) at 3010 cm^{-1} of which the latter two are significantly higher than the corresponding modes of the acetylide. The disappearance of the 1290-cm^{-1} carbon–carbon stretching mode of acetylide upon annealing to 500 K also assists us in distinguishing acetylide and methylidyne. The mode at 570 cm^{-1} in Figure 5c is the carbon–metal stretching mode of carbon adatoms and/or carbon dimers. The broad feature at 1100–1600 cm^{-1} may be attributed to the carbon–carbon stretching mode of these dimers. The vibrational modes of the methylidyne are compared in Table V to those of high-temperature ($T > 400$ K) methylidynes on various transition-metal surfaces, as well as tricobalt and triruthenium μ_3-CH complexes.[1,2,4,9,10,50-53] Our assignments agree quite well with those of methylidyne adsorbed on the Fe(111), Ni(111), and Pd(111) surfaces and are consistent with those of the organometallic complexes. The isotopic shifts of the vibrational modes of methylidyne adsorbed on Ru(001) are also in agreement with those of $(CO)_4Co_3(\mu_3\text{-}CD)$.

All of the methylidyne modes are eliminated by annealing the Ru(001) surface above 700 K. After this annealation, weak modes near 600 and 1100–1600 cm^{-1} are observed which are attributed to ν(RuC) of carbon adatoms and dimers and ν(CC) of carbon dimers. These modes are present in the EEL spectra of both C_2H_4 and C_2D_4. No other features are present in the high-temperature EEL spectra, supporting the thermal desorption results which show complete desorption of hydrogen (and ethylene) below 700 K.

Bearing in mind what we have learned from EELS concerning the decomposition of ethylene on Ru(001), we now return to a more detailed analysis of the thermal desorption spectra. In the case of ethylene adsorbed on the Ru(001) surface, three reactions generate surface hydrogen below 400 K, namely, (1) C_2H_4 dehydrogenation to CCH(a) and 3H(a), beginning at 150 K; (2) C_2H_4 dehydrogenation to CCH_3(a) and H(a), also beginning at 150 K; and (3) CCH_3 decomposition to 2C(a) or C_2(a) and 3H(a), beginning at 330 K. As shown in Figure 1b, a large ethylene exposure produces a sharp peak at 355 K with a shoulder near 400 K in the hydrogen thermal desorption spectrum, followed by a long, high-temperature tail. Since the high-temperature tail corresponds exclusively to methylidyne decomposition and represents a small fraction of the total hydrogen that is desorbed (approximately 10%), a hydrogen mass balance requires that the desorption which occurs below 500 K corresponds to surface hydrogen from acetylide and ethylidyne formation as well as from ethylidyne decomposition.

For rather low exposures of ethylene, below 0.6 langmuir, the hydrogen thermal desorption spectra are quite different, although the EEL spectra of all coverages of ethylene adsorbed on Ru(001) are qualitatively the same. The thermal desorption spectrum of hydrogen following a low ethylene exposure contains a prominent peak (which shifts as a function of coverage) and also a high-temperature tail (cf. Figure 1c). As shown by the EELS results, the tail corresponds to hydrogen desorption that is limited by methylidyne decomposition. The hydrogen desorbing in the major peak is due to surface hydrogen from ethylene decomposition to ethtylidyne and acetylide and ethylidyne decomposition to surface carbon, as is the hydrogen desorbing in the 355 K peak following higher ethylene exposures. The shift in this peak as a function of ethylene coverage indicates that the desorption of this hydrogen is desorption-limited. This is confirmed by experiments conducted on the carbonaceous residue that remains after annealing to 700 K the ruthenium surface which had been exposed to 0.4 langmuir of C_2H_4 at 100 K. Hydrogen was adsorbed on this carbonaceous residue at 90 K, and then a thermal desorption measurement was carried out. The thermal desorption spectra showed that the major hydrogen thermal desorption peak was repopulated, confirming that this peak is due to desorption of surface hydrogen.

The sharp peak at 355 K in the thermal desorption spectra of hydrogen following an exposure of ethylene *exceeding* 0.6 langmuir consists of surface hydrogen formed from ethylene decomposition at lower temperatures (150–280 K) and driven by the presence of that hydrogen from ethylidyne decomposition. The maximum rate of the latter occurs at 355 K. The high-temperature shoulder on this peak (near 400 K) corresponds to desorption of residual surface hydrogen. That the sharp peak at 355 K and its high-temperature shoulder are derived from surface hydrogen has been confirmed by hydrogen postadsorption experiments. First, the Ru(001) surface was exposed to 5 langmuir of C_2H_4 at 90 K, annealed to 800 K, cooled to 90 K, and exposed to 30 langmuir of hydrogen. A subsequent thermal desorption spectrum (Figure 6b) shows a peak at 355 K with a high-temperature shoulder.[54] A comparison with the hydrogen thermal desorption spectrum after an exposure to 5 langmuir of C_2H_4 (Figure 6a) shows that less hydrogen is present in the 355 K peak of Figure 6b and that the leading edge of the peak in this spectrum is not so sharp. These differences are due solely to the presence of ethylidyne decom-

(47) Parmeter, J. E.; Hills, M. M.; Weinberg, W. H. *J. Am. Chem. Soc.*, following paper in this issue.
(48) Kesmodel, L. L. *Vac. Sci. Technol., A* **1984**, *2*, 1083.
(49) Kesmodel, L. L.; Wadill, G. D.; Gates, J. A. *Surf. Sci.* **1984**, *138*, 464.
(50) Demuth, J. E.; Ibach, H. *Surf. Sci.* **1978**, *78*, L238.
(51) Erley, W.; McBreen, P. H.; Ibach, H. *J. Catal.* **1983**, *84*, 229.
(52) Oxton, I. A. *Spectrochim. Acta, Part A* **1982**, *38*, 181.
(53) Howard, M. W.; Kettle, S. F.; Oxton, I. A.; Powell, D. B.; Sheppard, N.; Skinner, P. *J. Chem. Soc., Faraday Trans 2* **1981**, *77*, 397.

(54) EEL spectra of this adlayer support the presence of only carbon and hydrogen adatoms; in particular, no modes of methylidyne are observed.

Table V. Comparison of Vibrational Frequencies of Surface Methylidyne Species to Those of $(CO)_4Co_3(\mu_3\text{-CH})$ and $(CO)_9H_3Ru_3(\mu_3\text{-CH})$

mode	CH on Ru(001)	CH on Fe(111)[2]	CH on Fe(110)[1,50]	CH on Ni(111)[4,51]	CH on Pd(111)[9,10]	$(CO)_9H_3Ru_3$-$(\mu_3$-CH)[52]	$(CO)_4Co_3$-$(\mu_3$-CH)[53]
ν(CH)	3010	3015	3050	2980	3002	2988	3041
δ(MCH) (e)	810	795	880	790	762	894	850
ν_s(MC) (a_1)	465					670	715
ν_a(MC) (e)	n.r.					424	417
ν(CD)	2250						2268
δ(MCD) (e)	615						680
ν_s(MC) (a_1)	415						696
ν_a(MC) (e)	n.r.						410

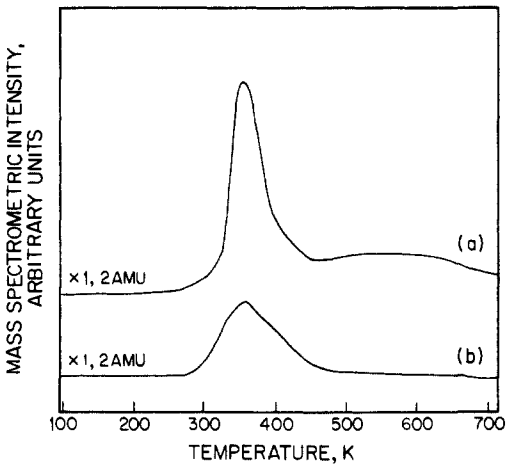

Figure 6. Hydrogen thermal desorption following (a) exposure of 5 langmuir of C_2H_4 and (b) exposure of 5 langmuir of C_2H_4 followed by annealing to 800 K, cooling to 90 K, and exposure to 30 langmuir of H_2.

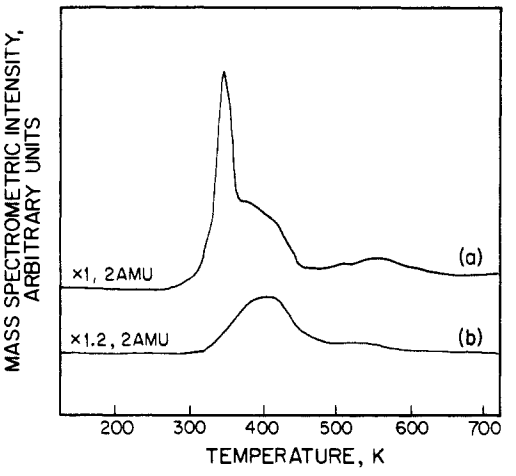

Figure 7. Hydrogen thermal desorption following exposures of (a) 0.4 langmuir of C_2H_4 followed by 2 langmuir of H_2 and (b) 0.4 langmuir of C_2H_4 at 100 K.

position in Figure 6a and its absence in Figure 6b.

In a second experiment, the ruthenium surface was exposed to 0.4 langmuir of C_2H_4, followed by 1 langmuir of H_2 at 90 K. A subsequently measured hydrogen thermal desorption spectrum (Figure 7a) was unlike that following an exposure of 0.4 langmuir of C_2H_4 (Figure 7b). Rather, it appears qualitatively similar to that observed after an exposure of 1 langmiur of C_2H_4 (cf. Figure 1b) in that both spectra contain sharp peaks at 355 K. The major difference between the two spectra of Figure 7 is that more hydrogen adatoms are present in spectrum a, and this is reflected in the much more prominent high-temperature shoulder. Furthermore, more ethylidyne is formed relative to acetylide following the postadsorption of hydrogen, suggesting that this branching ratio is a function of hydrogen coverage. This will be discussed in greater detail in section IV.

To summarize, at all coverages ethylene adsorbes in a di-σ-bonded configuration that decomposes to ethylidyne, acetylide, and surface hydrogen above 150 K. The ethylidyne dehydrogenates above 330 K, generating additional surface hydrogen. The surface hydrogen desorbs at a temperature which decreases with increasing coverage following ethylene exposures below 0.6 langmuir and at 355 K following higher exposures of ethylene. The acetylide decomposes to carbon adatoms and methylidyne near 380 K. Finally, methylidyne decomposes, evolving hydrogen, after annealing above 500 K. For exposures of ethylene below 0.6 langmuir, complete decomposition of methylidyne occurs below 600 K. For higher ethylene exposures, the carbon adatoms (which are present in a higher concentration on the surface) stabilize the methylidyne, such that methylidyne decomposition extends up to 700 K. A plot of ethylene coverage as a function of ethylene exposure as well as a plot of the fractional coverage of ethylene which desorbs molecularly as a function of ethylene exposure is presented in Figure 8.

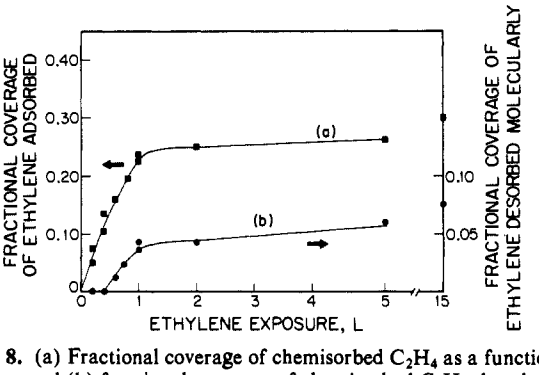

Figure 8. (a) Fractional coverage of chemisorbed C_2H_4 as a function of exposure and (b) fractional coverage of chemisorbed C_2H_4 that desorbs molecularly as a function of exposure. The temperature of adsorption is 80 K.

IV. Discussion

As described in section III, ethylene chemisorbs on the Ru(001) surface in a di-σ-bonded configuration (at a surface temperature below 150 K) and at 80 K condenses into a molecular multilayer that resembles the free ethylene molecule (cf. Table I). As may be seen in Figure 2, all five IR-active modes of ethylene appear in the EEL spectra of the molecular multilayer. In addition, the carbon–carbon stretching mode, the CH_2 rocking mode, and the asymmetric CH_2 scissoring mode were resolved in some spectra. These modes are excited via an impact scattering mechanism.

Chemisorbed ethylene, which is stable below 150 K, is di-σ-bonded to the Ru(001) surface, and assignments of the observed vibrational modes are listed in Table II. This molecularly chemisorbed ethylene on the Ru(001) surface appears to undergo a somewhat greater degree of rehybridization than it does on the

Ni(110), Ni(111), and Fe(110) surfaces.[1,3-5] The differences in frequency between the CH_2 twisting and scissoring modes of C_2H_4 on Ru(001) and on Fe(111) are not unexpected since ethylene on Fe(111) is severely tilted with respect to the surface plane such that two hydrogens are subject to multicenter interactions, which are mainfested by a softened ν(CH) mode at 2725 cm^{-1}.[2] This distorted geometry downshifts both the CH_2 wagging and scissoring modes.

Rather little can be said conclusively concerning the symmetry of the di-σ-bonded ethylene on Ru(001). Application of the dipolar selection rule would imply that the symmetry of the adsorbate–substrate complex is C_1, since both the CH_2 rocking and twisting modes appear in figure 3a. However, EEL spectra measured off-specular show that these modes are largely impact excited, and therefore, the dipolar selection rule does not apply. Hence, the symmetry of di-σ-bonded ethylene on Ru(001) remains indeterminant. A near-edge X-ray absorption fine structure (NEXAFS) study of ethylene adsorbed on Pt(111) at 90 K by Horsley and co-workers[55] has shown that ethylene is symmetrically di-σ-bonded to two platinum atoms with the carbon–carbon bond axis parallel to the surface and a carbon–carbon bond length of 1.49 ± 0.03 Å. We expect that di-σ-bonded ethylene would be adsorbed similarly on the Ru(001) surface.

Barteau et al.[22] have reported a di-σ-bonded ethylene species on Ru(001) with a carbon–carbon stretching mode at 1330 cm^{-1}. Our results indicate that their assignments are incorrect, however, for the following reasons. First, they adsorbed ethylene at 170 K, a temperature at which we have shown that di-σ-bonded C_2H_4 has begun to decompose forming a mixed overlayer of C_2H_4(a), CCH_3(a), CCH(a), and H(a). Thus the modes they identify as resulting from di-σ-bonded C_2H_4 are in fact a combination of di-σ-bonded C_2H_4, CCH_3, and CCH modes. The 1330-cm^{-1} loss which they assign to ν(CC) is actually the $\delta_s(CH_3)$ mode of ethylidyne. This feature becomes more intense with further annealing which decomposes the C_2H_4(a) and produces more ethylidyne. Second, our EEL spectra of C_2D_4 on Ru(001) annealed at 170 K show clearly that the previous assignment[22] is incorrect, because the 1330-cm^{-1} loss downshifts to 1000 cm^{-1} in the deuterated spectra, and there are no modes of comparable intensity to the 1300-cm^{-1} mode between 1150 and 2190 cm^{-1} in the deuterated spectra. Barteau and co-workers[22] did not measure any EEL spectra of deuterated ethylene and thus could not distinguish carbon–carbon vibrational modes from hydrogen modes. A comparison of the EEL spectra of C_2H_4 and C_2D_4 is essential to the correct identification of these vibrational modes. As shown in Tables II–IV, EEL spectra of C_2D_4 on Ru(001) annealed between 110 and 400 K confirm our mode assignments for the three adspecies, di-σ-bonded ethylene, ethylidyne, and acetylide. Finally, we note that a carbon–carbon stretching frequency of 1040 cm^{-1} is more reasonable than one of 1330 cm^{-1} for an sp^3-hybridized hydrocarbon species, and it is consistent with the carbon–carbon stretching mode observed at 1135 cm^{-1} for acetylene chemisorbed on Ru(001).[47] It would be expected that ν(CC) of chemisorbed ethylene on Ru(001) would be lower than this value, ruling out the assignment of the 1145-cm^{-1} mode to ν(CC) of C_2H_4. Furthermore, the 1145-cm^{-1} mode shifts considerably (to 900 cm^{-1}) in the spectra of C_2D_4 and certainly cannot be due to ν(CC).

No LEED patterns other than the (1 × 1) of the substrate were observed for the ethylene overlayer between 90 and 300 K. Hence LEED measurements cannot aid in a determination of the ethylene surface structure or absolute coverages. However, thermal desorption results for C_2H_4 and H_2 have been used to estimate the ethylene coverage using the known saturation fractional coverage of hydrogen (0.85).[32] The ethylene coverage (excluding the multilayer) is presented as a function of ethylene exposure in Figure 8a. From this figure, we see that the saturation (fractional) coverage of chemisorbed ethylene is approximately 0.30. Figure 8a was used also to obtain the initial probability of adsorption of ethylene at 100 K, which was found to be unity within the limits of experimental uncertainty. The activation energy of desorption (equal to the heat of adsorption) of di-σ-bonded C_2H_4 was estimated from the thermal desorption measurements. When the method of Redhead[56] is used and a preexponential factor of 10^{13}–10^{14} s^{-1} is assumed, a value of approximately 11.6 ± 1 kcal/mol is obtained. Considering the changes in bond strengths due to rehybridization of the carbon atoms, we have also estimated that the binding energy of di-σ-bonded ethylene is between 105 and 135 kcal/mol. *Thus the observation of a low heat of adsorption for chemisorbed ethylene on Ru(001) does not imply that the ruthenium–carbon bond is weak.*

When the saturated overlayer of chemisorbed ethylene is annealed to 250 K, approximately 20% of the ethylene desorbs, while the remainder dehydrogenates to ethylidyne, acetylide, and surface hydrogen. The stoichiometry of the ethylidyne formed by ethylene decomposition on Pt(111) was confirmed by hydrogen thermal desorption spectra in which approximately 25% of the total hydrogen desorbed from the surface at 300 K, the same temperature at which ethylidyne was shown to form via EELS.[57] Unfortunately, the hydrogen from ethylidyne formation remains adsorbed on the Ru(001) surface, ultimately desorbing with hydrogen from ethylidyne decomposition. Hence we are unable to confirm *directly* the stoichiometry of the ethylene decomposition products from hydrogen thermal desorption spectra. The ethylidyne on Ru(001) begins to decompose at approximately 330 K, whereas the ethylidyne formed on Pt(111) is stable to 400 K.[7] The reduced stability of ethylidyne on Ru(001) is undoubtedly due to the stronger metal–hydrogen and metal–carbon bonds formed on the ruthenium surface, which makes the decomposition of ethylidyne via metal–hydrogen and metal–carbon bond formation more favorable both thermodynamically and kinetically.

The identification of ethylidyne and acetylide as the decomposition products of di-σ-bonded ethylene on Ru(001) can be contrasted to the results of Barteau et al.[22] who only identified ethylidyne. We also note that Barteau assigned the $\rho(CH_3)$ mode of ethylidyne to a loss at 870 cm^{-1}. We observed no such mode in our EEL spectra and cannot account for this discrepancy but merely mention that our assignment of the 1000-cm^{-1} loss to $\rho(CH_3)$ and the observed isotopic shift to 800 cm^{-1} for $\rho(CD_3)$ are in agreement with the frequencies observed for other ethylidyne species.

Our EEL spectra of the thermal evolution of ethylidyne and acetylide on Ru(001) and complementary thermal desorption spectra show that virtually all of the ethylidyne dehydrogenates to surface carbon below 360 K, leaving only CCH(a) and H(a) on the surface. Thus an EEL spectrum measured after annealing to 360 K (Figure 5b) contains only the loss features of acetylide, permitting unambiguous identification of this intermediate. The observation of the carbon–hydrogen bending mode of acetylide at 280 K, prior to the onset of ethylidyne dehydrogenation, implies that acetylide is not a decomposition product of ethylidyne. Further proof of this assertion comes from CO and C_2H_4 coadsorption experiments.[58]

By analogy to all relevant organometallic ethylidyne complexes synthesized to date, it is almost certain that the carbon–carbon bond axis of ethylidyne on Ru(001) is very nearly perpendicular to the surface. This configuration is also supported by the strong intensity of the ν(CC) mode of ethylidyne at 1140 cm^{-1} in the EEL spectrum of Figure 5a and its predominantly dipolar character. Furthermore it is very probable that ethylidyne is bonded to the Ru(001) surface in a threefold hollow site both by analogy to the trimetal μ_3-CCH_3 complexes[45,46] and because ethylidyne has been observed only on hexagonal surfaces.[4,7,16] A further indication of this bonding of ethylidyne on Ru(001) is provided by NEXAFS results of ethylidyne on Pt(111),[55] which showed that the ethylidyne is symmetrically bonded to three

(55) Horsley, J. A.; Stöhr, J.; Koestner, R. J. *J. Chem. Phys.* **1985**, *83*, 3146.

(56) Redhead, P. A. *Vacuum* **1962**, 203.

(57) Ibach, H.; Mills, D. L. *Electron Energy Loss Spectroscopy and Surface Vibrations*; Academic: New York, 1982.

(58) Hills, M. M.; Parmeter, J. E.; Weinberg, W. H., unpublished results.

platinum atoms with the carbon–carbon bond axis essentially perpendicular to the surface.

Next, we consider the effects of simultaneous ethylidyne decomposition and hydrogen desorption on the observed shape of the hydrogen thermal desorption peak. When the Ru(001) surface on which ethylene is adsorbed (exposures above 0.6 langmuir) is annealed to 300 K, hydrogen desorption is observed. In these measurements, hydrogen desorbs at this low temperature due to its higher surface coverage. As the overlayer is annealed to 330 K, additional hydrogen desorbs, and ethylidyne begins to dehydrogenate, replenishing the supply of surface hydrogen. Thus adjacent to the decomposing ethylidyne, an area of high local density of hydrogen adatoms is formed, which accelerates the rate of desorption of hydrogen and gives the hydrogen thermal desorption peak a sharp leading edge. Comparing Figure 6a and 6b, it is clear that the high-temperature shoulder on the 355 K hydrogen thermal desorption peak results from residual surface hydrogen.

For these higher exposures of ethylene, the temperature of the hydrogen thermal desorption peak remains at 355 K independent of coverage. Ethylidyne decomposition dictates this hydrogen desorption since the desorption of hydrogen occurs at a lower temperature in a broader peak at higher hydrogen adatom coverages (from the adsorption of hydrogen). The adsorption and decomposition of ethylene at high coverages is otherwise identical with that for lower coverages with three exceptions. First, a multilayer of ethylene forms which desorbs at 110 K. Second, some of the di-σ-bonded ethylene desorbs (cf. Figure 8b). Finally, the ratio of ethylidyne to acetylide that is formed is increased. Recall that annealing to 400 K the Ru(001) surface on which ethylene is adsorbed not only decomposes the ethylidyne but also causes cleavage of the carbon–carbon bond of the acetylide, leaving methylidyne and carbon adatoms. The high-temperature tail of the hydrogen thermal desorption peak after ethylene adsorption corresponds to dehydrogenation of methylidyne. Consequently, the ratio of ethylidyne to acetylide that is formed from ethylene can be obtained from the relative areas of the 355 K peak and the tail. The acetylide coverage is equal to the coverage of the hydrogen desorbing in the high-temperature tail. The ethylidyne coverage is obtained by subtracting 3 times the acetylide coverage from the coverage of hydrogen desorbing in the 355 K hydrogen thermal desorption peak and its high-temperature shoulder and dividing this number by four. We find that a saturation exposure of ethylene decomposes to ethylidyne and acetylide in the approximate ratio of 60:40, whereas a lower exposure, 0.4 langmuir of C_2H_4, yields a ratio of 50:50. Consequently ethylidyne formation is favored at higher surface coverages. This result may be interpreted in terms of the number of hydrogen adatoms generated by ethylene decomposition to ethylidyne (one per C_2H_4) vs. acetylide (three per C_2H_4). At higher surface coverages, more threefold sites, required for hydrogen adatoms, will be either occupied or blocked. Also, the coverage of hydrogen will be greater as ethylene dehydrogenation proceeds. Thus, the decomposition product that requires fewer vacant surface sites for formation and is composed of more hydrogen atoms, ethylidyne, is favored. The dependence of the ratio of ethylidyne to acetylide formed upon the hydrogen coverage has also been confirmed by hydrogen thermal desorption experiments measured following a saturation ethylene exposure at 350 K. At this temperature, the hydrogen adatom concentration on the surface is reduced. This lower hydrogen coverage caused the acetylide coverage to increase by approximately 50% compared to the coverage of acetylide formed following a saturation ethylene exposure at 80 K, and annealing to 350 K, as judged by the relative intensities of the high-temperature tails in the hydrogen thermal desorption spectra.

Finally, we discuss briefly the mechanism of dehydrogenation of ethylidyne. The EEL spectra measured immediately following the decomposition of ethylidyne show no enhancement of the carbon–hydrogen bending mode of acetylide and provide no evidence for methylidyne formation. Thus, we can rule out both acetylide and methylidyne formation from ethylidyne decomposition and conclude that ethylidyne must dehydrogenate completely to either carbon–carbon dimers [with ν(CC) at 1100–1600 cm^{-1} in the EEL spectra of Figure 5b and 5c] and hydrogen or carbon adatoms and hydrogen. The observed complete dehydrogenation of ethylidyne at a temperature at which acetylide is stable on the surface is quite important. It implies that the reaction coordinate that results in the loss of the first hydrogen atom from ethylidyne is not the one which would lead to the stable surface acetylide. A plausible but most certainly speculative scenario for the dehydrogenation of ethylidyne would involve interaction with an adjacent threefold hollow site, whereas the stable acetylide (almost certainly not oriented parallel to the surface plane) has a structure that is rotated 60° with respect to this reaction coordinate.

V. Conclusions

Ethylene chemisorbs on Ru(001) in a di-σ-bonded configuration at temperatures below approximately 150 K. When heated, competing molecular desorption, dehydrogenation to acetylide, and dehydrogenation to ethylidyne occur. The resulting thermal decomposition scheme for a saturation coverage of chemisorbed ethylene (θ = 0.30) may be depicted as

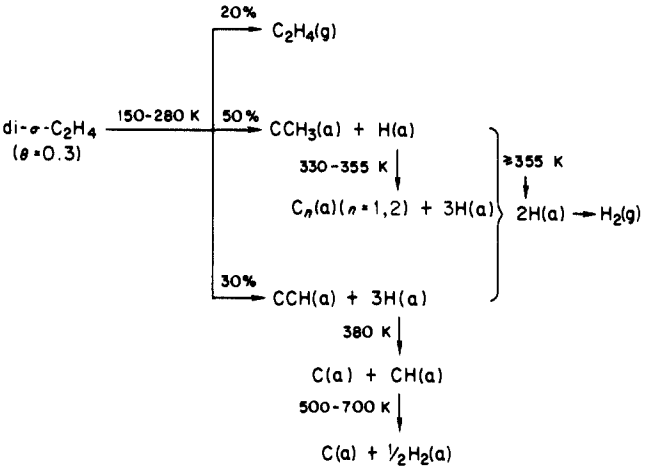

The ethylidyne formed on Ru(001) is less stable than on other groups 8–10 metal surfaces; e.g., it begins to decompose to carbon and hydrogen adatoms near 330 K compared to the decomposition temperature of approximately 400 K observed on Pt(111) and Rh(111). Carbon–carbon bond cleavage of the acetylide occurs at 380 K, producing surface carbon and methylidyne of which the latter dehydrogenates between 500 and 700 K. Following ethylene exposures exceeding 0.6 langmuir, desorption of hydrogen occurs in a sharp peak with a maximum rate of desorption at 355 K, which is limited by ethylidyne decomposition, in a shoulder at approximately 400 K on this peak due to desorption-limited hydrogen and also in a high-temperature tail due to methylidyne decomposition. Hydrogen desorption following lower ethylene exposures becomes desorption-limited, except for the hydrogen that is evolved from the decomposition of methylidyne.

To summarize, ethylene adsorbed on Ru(001) produces both ethylidyne and the more extensively dehydrogenated acetylide. Thus, the behavior of ethylene adsorbed on Ru(001) appears to be intermediate between the more complete dehydrogenation observed on Ni(111) and Co(001) and the exclusive formation of the less dehydrogenated stable ethylidyne species found on the hexagonal surfaces of rhodium, palladium, and platinum.

Acknowledgment. This work was supported by the National Science Foundation under Grant CHE-8516615. Acknowledgment is also made to the donors of the Petroleum Research Fund, administered by the American Chemical Society, for the partial support of this research.

Registry No. C_2H_4, 74-85-1; Ru, 7440-18-8; CCH_3, 67624-57-1; CCH, 29075-95-4; CH, 3315-37-5.